Biochemistry

pubs.acs.org/biochemistry Article

Hysteresis in Hepatitis B Virus (HBV) Requires Assembly of Near-Perfect Capsids

Caleb A. Starr, Lauren F. Barnes, Martin F. Jarrold, and Adam Zlotnick*

Cite This: *Biochemistry* 2022, 61, 505−513 Read Online

ABSTRACT: The hepatitis B virus (HBV) must release its contents to initiate infection, making capsid disassembly critical to the viral life cycle. Capsid assembly proceeds through a cascade of weak interactions between copies of capsid protein (Cp) to yield uniform particles. However, there is a hysteresis to capsid dissociation that allows capsids to persist under conditions where they could not assemble. In this study, we have sought to define the basis of hysteresis by examining urea-induced dissociation of *in vitro*-assembled HBV capsids. In general, capsid samples show a mixture of two pools, differentiated by stability. Labile capsid dissociation corresponds to an ∼5 μM pseudocritical concentration of assembly (pcc), the same as that observed in assembly reactions. Dissociation of the stable pool corresponds to a subfemtomolar pcc, indicative of hysteresis. The fraction of stable capsids in an assembly reaction increases with the integrity of the Cp preparation and when association is performed at a higher ionic strength, which modifies the Cp conformation. Labile complexes are more prevalent when assembly conditions yield many kinetically trapped (incomplete and overgrown) products. Cp isolated from stable capsids reassembles into a mixture of stable and labile capsids. These results suggest that hysteresis arises from an ideal capsid lattice, even when some of the substituents in that lattice have defects. Consistent with structural studies that show a subtle difference between Cp dimers and Cp in capsid, we propose that hysteresis arises when HBV capsids undergo a lattice-dependent structural transition.

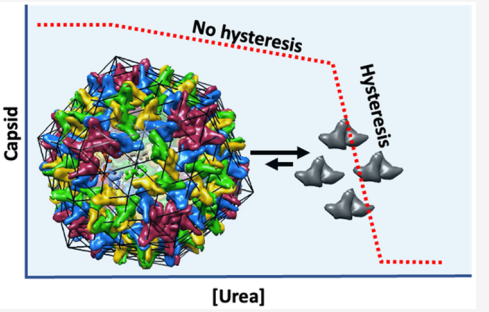

The hepatitis B virus (HBV) is an icosahedral, partially double-stranded DNA virus that poses a global health problem.[1] As of 2019, ∼1.5 million people are infected yearly by HBV and 820,000 people die yearly from liver failure, cirrhosis, and hepatocellular carcinoma resulting from HBV infection.[2] A vaccine protects against new infection, and there are therapeutics to control HBV; however, there is no cure for chronic HBV.

In the HBV life cycle, the capsid or core protein (Cp) plays a role in almost every step.[3] Capsids assemble around an RNA transcript of the viral genome and viral polymerase, act as a metabolic compartment for reverse transcription, traffick within a cell, and bind surface protein to obtain an envelope for secretion or deliver their mature genome to the nucleus. As important as capsid assembly is to the HBV infection cycle so too is capsid disassembly. Each infectious particle must go on to successfully disassemble during infection to continue the HBV life cycle.[4] The HBV disassembly process and mechanism have been studied little relative to HBV assembly. The details of the disassembly process also have implications for better understanding HBV capsid thermodynamics and stability. For nearly two decades, it has been established that HBV exhibits a hysteresis to disassembly.[5] An indication of hysteresis in the context of HBV is that the energy of disassembly is much greater than the energy of assembly. Once the HBV capsid is fully formed, it is very difficult to disassemble *in vitro*.

The wild-type HBV Cp is a homodimer in which each subunit has 183 amino acids (Cp183), which comprise the dimer-forming assembly domain and the arginine-rich C-terminal domain. For *in vitro* studies, it is common to truncate the Cp to 149 amino acids (Cp149), eliminating the C-terminal domain and thereby isolating protein−protein interactions. Cp183 and Cp149 dimers are very stable and do not measurably dissociate in solution.[6] Cp183 and Cp149 self-assemble into T = 4 capsids (∼95%) and T = 3 capsids (∼5%).[7] In assembly reactions, the assembly association energy can be characterized by a pairwise contact energy ($\Delta G_{contact}$) between a pair of dimers or a pseudocritical concentration (pcc), analogous to a critical micellar concentration (see the equations in Methods).[8] The $\Delta G_{contact}$ is approximately −3.4 kcal/mol at a physiological ionic strength,[9]

Received: December 18, 2021
Revised: February 23, 2022
Published: March 8, 2022

https://doi.org/10.1021/acs.biochem.1c00810
Biochemistry 2022, 61, 505−513

Table 1. Parameters for Dissociation Curves[a]

figure, sample, phase	$\Delta G_{contact,disassembly}$ (kcal/mol)	pseudocritical concentration (pcc) (M)	mole fraction
Figure 2, sonicator dimer, low urea	−3.4 ± 0.01	4.9×10^{-6}	0.60
Figure 2, sonicator dimer, high urea	−13.0 ± 0.35	3.1×10^{-20} (10^{-17} to 10^{-23})	0.40
Figure 2, emulsifier dimer, low urea	−3.7 ± 0.01	1.7×10^{-6}	0.25
Figure 2, emulsifier dimer, high urea	−10.5 ± 0.98	2.0×10^{-16} (10^{-15} to 10^{-17})	0.75
Figure 5A, 150 mM NaCl, low urea	−3.6 ± 0.06	1.10×10^{5}	0.20
Figure 5A, 150 mM NaCl, high urea	−11.2 ± 0.39	1.92×10^{16}	0.80
Figure 5A, 300 mM NaCl, low urea	−4.1 ± 0.09	6.04×10^{5}	0.20
Figure 5A, 300 mM NaCl, high urea	−8.0 ± 0.27	3.55×10^{11}	0.80
Figure 5A, 500 mM NaCl, low urea	−4.1 ± 0.03	6.04×10^{5}	0.40
Figure 5A, 500 mM NaCl, high urea	−9.9 ± 0.35	2.29×10^{14}	0.60
Figure 6, 1% V124A, low urea	−3.4 ± 0.04	5.56×10^{4}	0.30
Figure 6, 1% V124A, high urea	−7.7 ± 0.40	1.28×10^{11}	0.70
Figure 6, 10% V124A, low urea	−3.8 ± 0.10	2.17×10^{5}	0.25
Figure 6, 10% V124A, high urea	−7.1 ± 0.33	1.65×10^{10}	0.75
Figure 6, 50% V124A	−3.7 ± 0.04	1.55×10^{5}	1
Figure 6, 100% V124A	−4.6 ± 0.84	3.31×10^{6}	1

[a] $\Delta G_{contact}$ values are calculated (eq 3) from the capsid and dimer concentrations, assuming equilibrium. The calculated pseudocritical concentration (eq 4) is equivalent to the amount of free dimer left in solution in an equilibrated assembly reaction mixture. A range is provided for several high-urea phases. The mole fraction is the fraction of the input capsids in the low- or high-urea phases of dissociation.

corresponding to a millimolar dissociation constant. Because each subunit is tetravalent and the interactions are pairwise, the pcc is proportional to twice the $\Delta G_{contact}$,[10] or ∼15 μM. At Cp concentrations below the pcc, very little dimer assembles, while almost all Cp above the pcc is found in the form of capsid.[9,11] Though assembled from weak dimer−dimer interactions,[9] HBV capsids can be purified and stored at very low concentrations for months without exchange of subunits with subunits.[12] This *in vitro* hysteresis has important implications *in vivo* where a virus must stay intact when between hosts.

In vitro disassembly of HBV capsids requires the addition of chaotropes such as guanidinium hydrochloride or urea to disrupt the hydrophobic dimer−dimer contacts.[6] Dilution of the capsids below the pcc is insufficient for disassembly.[5] Utilizing a chaotrope for disassembly also allows us to analogously apply established thermodynamic analyses for protein denaturation to our study of HBV disassembly.[13] Protein unfolding can be carried out by titrating the protein with a chaotrope, and the observed unfolding energy at a given chaotrope concentration can be extrapolated to zero chaotrope to obtain the calculated $\Delta G_{unfolding}$. We directly apply this analysis to HBV disassembly to obtain $\Delta G_{disassembly}$.

In this report, we show that HBV capsid disassembly can have two phases that had not been previously observed. The first phase appeared to be in equilibrium with free dimer and had no hysteresis, while the second phase contained capsids with a substantial hysteresis. Treating wild-type Cp149 capsids with modest urea concentrations caused flawed $T = 4$ capsids to dissociate and allowed isolation of highly stable capsids. We also found that highly stable capsid populations were enriched by assembly at a higher ionic strength, suggesting that flawed subunits could be cured by the kosmotropic effects of NaCl. The last part of this study sought to purposefully introduce defects into capsids by using a mutant with a weak association energy. We observed that small amounts of the mutant subunit had no effect, indicating the importance of the larger capsid lattice for regulating disassembly, while even capsids wholly composed of mutant subunits still exhibited some hysteresis.

METHODS

Protein and Capsid Preparation. The HBV capsid protein assembly domain, dimeric Cp149, was expressed in *Escherichia coli* and purified as previously described with minor modifications.[14] The final storage buffer for the Cp149 dimer consisted of 50 mM sodium bicarbonate (pH 9.5) and 1 mM dithiothreitol. The older protocol called for *E. coli* lysis via sonication. The resulting Cp149 dimer is termed the "sonicator dimer" throughout. The Cp149 purification protocol was modified to use an emulsifier (Avestin) to lyse the cells. This resulting Cp149 dimer is termed the "emulsifier dimer". For dissociation studies, capsids were assembled by diluting the Cp149 dimer to 25 μM in 300 mM NaCl, 50 mM Tris-HCl (pH 8), and 5 mM DTT at 4 °C and incubating for 24 h. Capsids were isolated from the unassembled dimer by size exclusion chromatography (SEC) using a Superose-6 column equilibrated in assembly buffer. Capsid fractions were pooled and concentrated using Amicon Ultra 15 centrifugal filters with 10 kDa cutoffs. Protein concentrations were determined by absorbance using an extinction coefficient of 60900 M^{-1} cm^{-1}.[14] Assembly at varying salt concentrations (150, 300, and 500 mM NaCl) was initiated, and capsids were resolved under the conditions described above.

Fluorescence Spectroscopy and Capsid−Dimer Equilibria. Tryptophan fluorescence spectra were recorded at 25 °C with a Photon Technology International (Irvine, CA) fluorometer using a 3 mm path length cuvette (Hellma, Forest Hills, NY). The excitation wavelength was 280 nm, and the fluorescence emission scans were conducted from 290 to 400 nm. For most single-wavelength experiments including urea titrations, we examined intrinsic fluorescence using a Synergy H1 or Neo2 plate reader (BioTek, Winooski, VT). All reactions utilized Greiner 96-well black, flat bottom, Fluotrac plates. Purified capsids were diluted to 10 μM in assembly buffer with urea added last to a final concentration adjusted in 0.1 M steps from 0 to 4 M. The intrinsic fluorescence for each reaction was recorded once per minute for 60 min. The excitation and emission wavelengths were 280 and 330 nm, respectively. After 60 min, plates were covered with aluminum

https://doi.org/10.1021/acs.biochem.1c00810
Biochemistry 2022, 61, 505−513

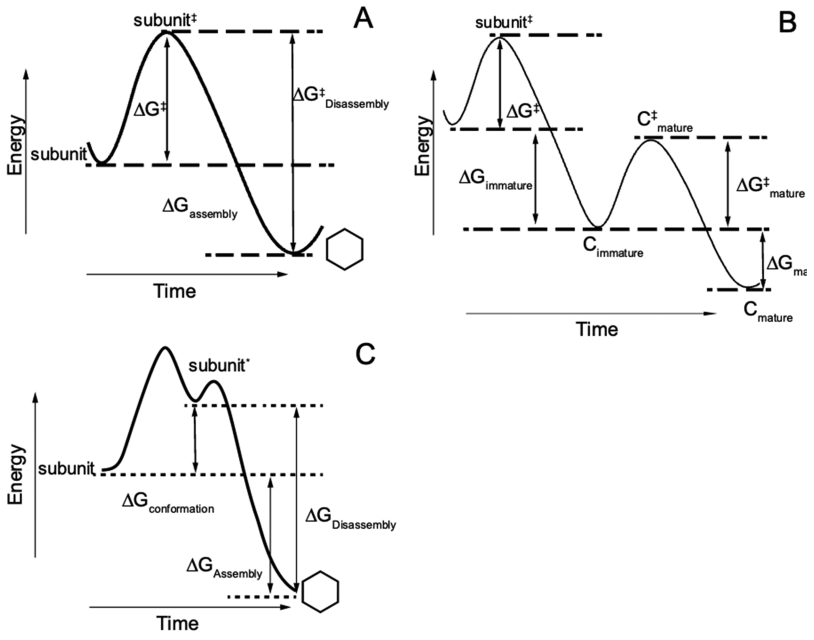

Figure 1. Thermodynamic working models for Cp149 capsid assembly and disassembly. (A) A simple model of capsid assembly describes a reaction in which no hysteresis is observed. Subunit goes through a transition state and assembles into capsid. The forward and reverse reactions are in equilibrium, and no hysteresis is expected. (B) A capsid maturation model describes an assembly reaction from subunit to immature capsid followed by a post-assembly maturation step, leading to hysteresis. (C) A subunit-based hysteresis model describes a reaction in which subunit must undergo an assembly active conformational change into subunit‡ before assembling into capsid. The difference in observation between capsid dissociating to subunit‡ or back to subunit leads to the observed hysteresis.

foil plate sealers, stored at room temperature, and then re-read at 24 h.

The fluorescence intensity for each sample was background subtracted and corrected for photobleaching. To correct for photobleaching, the slope of the plot of fluorescence versus time of the 0 M urea sample was used to correct the fluorescence intensity at all urea concentrations. Error bars are a standard deviation calculated from the average of three independent measurements. The corrected fluorescence at each urea concentration was assumed to be a sum of the capsid and dimer fluorescence and used to calculate K_{capsid}, $K_{contact}$, and $\Delta G_{contact,urea}$ (eqs 1−3).[5] The value for the pcc was calculated from $\Delta G_{contact}$ as described in eq 4.[10] The value for $\Delta G_{disassembly}$ was calculated by linearly extrapolating $\Delta G_{contact,urea}$ to 0 M urea. The error in Table 1 was calculated from the difference between the experimental data and the linear fits of the zero urea extrapolations.

$$K_{capsid} = \frac{[capsid]}{[Cp149]^{120}} \quad (1)$$

$$K_{contact} = \exp\left[\ln K_{capsid} - \ln\left(\frac{2^{119}}{120}\right)\right]/240 \quad (2)$$

$$\Delta G_{contact,urea} = -RT \ln(K_{contact,urea}) \quad (3)$$

$$pcc = K_{capsid}{}^{1/(1-120)} = \left(\frac{2^{119}}{120}\right)^{1/(1-120)} K_{contact}{}^{240/(1-120)} \quad (4)$$

SEC Analysis of Capsid−Dimer Equilibria. Purified capsids were diluted to 3, 5, or 10 μM in assembly buffer with final urea concentrations in 0.2 M steps from 0 to 4 M for 24 h. Reactions were resolved using a 21 mL Superose-6 column (GE) equilibrated in assembly buffer and mounted on a high-performance liquid chromatography (HPLC) instrument (Shimadzu). To evaluate assembly as measured by SEC, the capsid and dimer peaks were integrated and correlated with the total amount of protein injected onto the column. Error bars were derived from the average of three independent measurements. The resulting concentrations were used to calculate $\Delta G_{contact,urea}$ and $\Delta G_{disassembly}$ as described above.

Liquid Chromatography Mass Spectrometry (LCMS) Analysis of Cp149-V124A Co-assembled Capsids. Proteins were analyzed on a Synapt G2S device equipped with an iClass HPLC instrument (Waters Corp.). Buffer A consisted of 0.1% formic acid in water, and buffer B 0.1% formic acid in acetonitrile. Protein samples were injected and separated over a column [5 cm × 0.020 in. (inner diameter)] in-house packed with C4 resin (Jupiter 5 μm, Phenomenex) using a gradient from 5% to 100% B over 10 min. MS spectra were recorded every second in resolution mode. Spectra were deconvoluted using the MaxEnt1 algorithm.

Charge Detection Mass Spectrometry (CDMS) Analysis of Urea-Treated Cp149 Capsids. CDMS is a single-particle technique in which the mass of each individual ion is obtained by simultaneously measuring its mass-to-charge ratio (m/z) and charge. CDMS allows mass distributions to be measured for heterogeneous and high-molecular weight samples that cannot be measured by conventional MS. Here, CDMS was used to measure the mass distributions for Cp149 capsids that were treated with urea. CDMS instrumentation and methods have been described in detail elsewhere.[15−18] Briefly, samples were buffer exchanged into an ammonium acetate solution before being subjected to nanoelectrospray (Advion Triversa Nanomate). Ions enter the home-built CDMS instrument by ambient gas flow through a metal capillary. The ions pass through three differentially pumped

https://doi.org/10.1021/acs.biochem.1c00810
Biochemistry 2022, 61, 505−513

regions where they are separated from the ambient gas flow. They are then focused into an electrostatic linear ion trap (ELIT). The potentials on the end-caps of the ELIT are switched from transmission mode to trapping mode, and ions inside the ELIT are trapped. The trapped ions oscillate back and forth through a conducting cylinder, and the induced charge is detected by a charge sensitive amplifier. The resulting signal is digitized and transferred to a computer where it is analyzed by fast Fourier transforms (FFTs). The m/z is obtained from the oscillation frequency, and the FFT magnitude is proportional to the charge. Multiplying the m/z by the charge gives the mass of the ion. Measurements are performed for thousands of ions, and the masses are binned to give a mass spectrum.

RESULTS

Models of Hysteresis. HBV capsids have a characteristic hysteresis to dissociation: the association energy measured during an assembly reaction (per pairwise dimer−dimer interaction, $\Delta G_{contact,assembly}$) is much weaker than the dimer−dimer association energy measured during disassembly ($\Delta G_{contact,disassembly}$).[5] To explain hysteresis in HBV, we propose basic models describing capsid assembly and disassembly (Figure 1). In a simplest case model, no hysteresis is expected (Figure 1A). In this model, the capsid protein, "subunit", goes through a single transition state, subunit‡, associated with assembly into the capsid. This simplified diagram implicitly includes the 120 assembly reactants needed to build a $T = 4$ capsid. Capsid assembly reactions are steeply "downhill" because subunits are multivalent and the average number of contacts per subunit increases with each added subunit.[19] The simplified reaction coordinate shows assembly and disassembly reactions in equilibrium, and thus, no hysteresis to disassembly is expected. The observed association energy is $\Delta G_{assembly}$. The rate of assembly is proportional to $e^{\Delta G^{\ddagger}}$, and the rate of dissociation to $e^{\Delta G^{\ddagger}_{Disassembly}}$. Note that $\Delta G^{\ddagger}_{Disassembly}$ is equal to $\Delta G_{assembly} + \Delta G^{\ddagger}$. Dissociation of an icosahedral complex is more complex than depicted by this simple model, as capsid closure has the effect that every subunit makes the maximum number of contacts. Simulations of dissociation reactions showed that closure can contribute to a kinetic barrier to dissociation.[5] However, in those simulations, it is clear that biochemical modulation of assembly may have an outsize effect, leading to the following models.

The second model, the capsid maturation model, incorporates an additional step of postassembly maturation of the capsid (Figure 1B). This model can obviously be applied to those bacteriophages where capsid assembly is followed by a maturation reaction that involves a substantial change in conformation.[20−22] However, conformational changes need not be extremely obvious and may only be evident in energetic terms.[23] In the capsid maturation model, subunit assembles into an immature capsid, $C_{immature}$, which subsequently undergoes a maturation transition, advancing through the $C_{mature}^{\ddagger}$ transition state to the final mature form. The details of the transition state may be elaborate—consider a wave of conformational change across the maturing capsid—or purely entropic.[23,24] In this model, hysteresis to disassembly is observed because the observed energy of association is $\Delta G_{immature}$ and the apparent energy of dissociation is $\Delta G_{immature} + \Delta G_{mature}$.

A third model of hysteresis is based on a conformational change to the subunit prior to assembly. In this subunit-based model, a subunit in an assembly inactive state advances to an assembly active state (subunit*), which then assembles. The observed assembly reaction energy is then $\Delta G_{assembly}$; the cost of forming subunit* is not visible in $\Delta G_{assembly}$. The disassembly energy is the energy required to reach subunit* ($\Delta G_{conformation} + \Delta G_{assembly}$). This model is particularly attractive with HBV as it is consistent with the hypothesis that HBV Cp dimers undergo an allosteric transition to an assembly active state.[6,25−27]

Hysteresis and Heterogeneous Capsids. To differentiate these models with respect to HBV, we examined capsid stability during dissociation. During preparation of the core protein from *E. coli*, we initially isolate capsids, dissociate them by treatment with 3 M urea, reassemble the isolated Cp with a high NaCl concentration, isolate the resulting capsids (typically 40% of the input dimer), and then re-dissociate the capsid with 3 M urea to obtain the dimer. On the basis of its ability to assemble, we have considered the reassembled Cp dimer to be the "best" Cp; the resulting capsids can last months at refrigerator temperatures with little or no dissociation due to dilution.[5] However, we observed several recent HBV preparations yielded capsids that were more susceptible to dissociation. This observation gave us the opportunity to directly compare stable and labile capsids.

To quantify capsid dissociation and test for capsid heterogeneity, we examined urea titrations of the purified capsid by changes in the intrinsic Cp dimer fluorescence and integrated peak areas on SEC. Each Cp dimer contains eight tryptophan residues, and their intrinsic fluorescence approximately doubles when dimers are assembled into capsids. Chaotropes up to a threshold concentration, 4 M urea and 1.5 M guanidine HCl, result in reversible disassembly with little evidence of protein unfolding.[5,6,28]

We initially examined the capsid stability of two recent preparations of the Cp149 dimer, one prepared by lysing cells by sonication and the other by lysing cells with an emulsifier. For these experiments, capsid was assembled from both preparations by adjusting the NaCl concentration to 300 mM and allowing 24 h for equilibration prior to SEC purification. In the urea titrations, it was immediately evident that disassembly of Cp149 capsids took place in two distinct transitions (Figure 2A). The first, the low-urea phase, began around 0.8 M urea and ended at 2.5 M urea. The second, the high-urea phase, began around 2.5 M urea and ended around 3 M urea. To facilitate interpretation of dissociation of a 120-dimer complex, we calculated the association energy per dimer−dimer contact (described in Methods).[9] The free energy of disassembly from the titration, extrapolated to 0 M urea, $\Delta G_{disassembly,urea}$, was calculated for each phase (Figure 2B). The $\Delta G_{disassembly,urea}$ for the low-urea phases was −3.4 kcal/mol per dimer−dimer contact (Table 1). The high-urea phase for the sonicator dimer accounted for 40% of the protein with a $\Delta G_{disassembly,urea}$ of −13.0 kcal/mol per dimer−dimer contact. For the emulsifier dimer, the high-urea phase accounted for 75% of the proteins and had a $\Delta G_{disassembly,urea}$ value of −10.5 kcal/mol (Table 1). Thus, the emulsifier sample had almost twice as much high-urea capsid. We note that the energy for the low-urea transition is approximately the same as the association energy measured during assembly, corresponding to a pcc of ∼5 μM (Table 1), indicating that capsids in the first transition had no hysteresis to dissociation. Capsids from

https://doi.org/10.1021/acs.biochem.1c00810
Biochemistry 2022, 61, 505−513

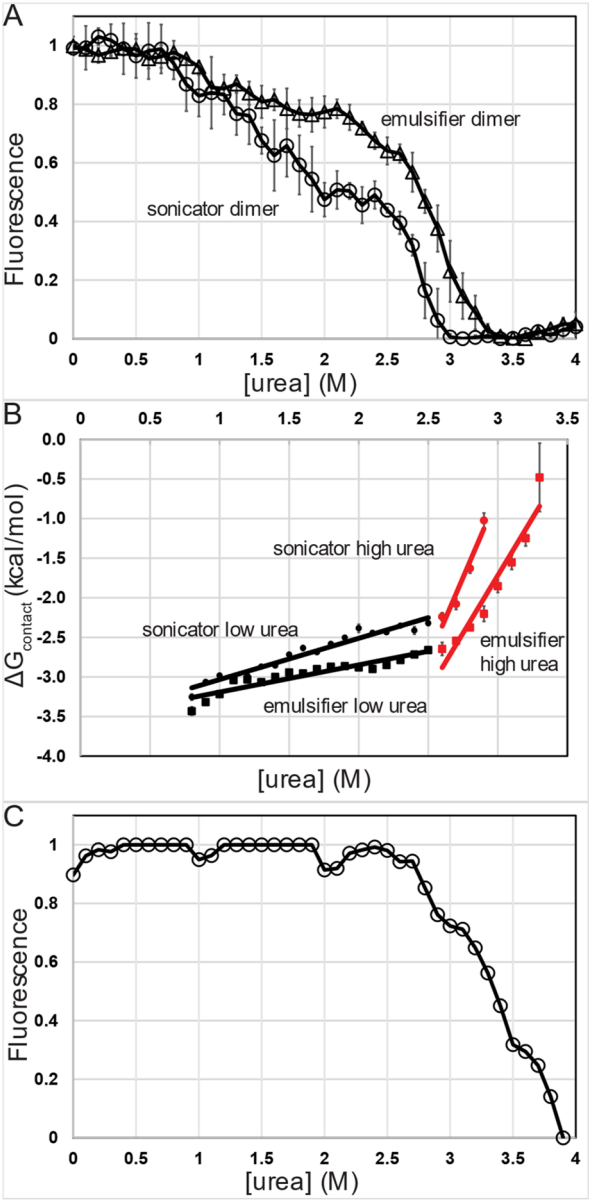

Figure 2. Cp149 capsid urea titrations. (A) Two capsid pools were subjected to increasing urea concentrations, and the amount of capsid remaining was measured using the intrinsic fluorescence. The fluorescence was plotted against the urea concentration to generate the disassembly curves shown. (B) Calculated $\Delta G_{contact,disassembly}$ for points in the disassembly transitions plotted vs urea concentration using the data from panel A. Extrapolation of each phase back to 0 M urea gives $\Delta G_{contact,disassembly}$ (Table 1). (C) Wild-type Cp149 capsids were incubated with 2.7 M urea to dissociate capsids from the low-urea phase and repurified to remove the excess dimer. The new capsid pool was used in a standard disassembly reaction and measured by fluorescence to generate the disassembly curve, which now shows a single phase.

the high-urea transition were markedly more stable, resulting in a sub-femtomolar calculated pcc.

We reasoned that a likely and testable explanation for two phases was that (i) a fraction of capsids had flawed subunits that led to unstable particles and (ii) the remaining robust capsids were enriched with the unflawed Cp149 dimer. It was striking that the gentler lysis technique, via an emulsifier, led to an improved yield of stable capsids. An alternative explanation for two phases in dissociation is that a subset of subunits was selectively removed from all capsids upon treatment with urea. To distinguish between these explanations, we examined capsids by charge detection mass spectrometry (CDMS), a single-molecule mass spectrometry technique. If the first explanation was correct, then we should be able to selectively dissociate capsids with flawed subunits and isolate robust capsids. If the second were correct, urea treatment should enrich the population of incomplete capsids. To accomplish this, Cp149 capsids assembled in 300 mM NaCl were treated with 2.7 M urea for 24 h and separated from the free dimer by SEC. When the resulting capsid pool was examined in a urea titration, the low-urea transition was conspicuously absent and a single, high-urea transition was observed (Figure 2C). CDMS demonstrated that capsids before and after treatment with 2.7 M urea displayed similar distributions of $T = 3$ and $T = 4$ particles (Figure 3). After urea treatment, capsids that were intermediate between $T = 3$ and $T = 4$ particles were depleted, indicating that urea treatment induced dissociation of $T = 4$ capsids with flaws and gaps. The high-mass tail on the $T = 4$ peak may be due to nonvolatile solutes (in particular, residual urea), ions, and water that remained associated with individual particles.

To test if the 2.7 M urea-treated capsids were enriched with subunits that formed highly stable capsids, the capsids were dissociated and the resulting dimers reassembled (Figure 4). It was immediately evident that two disassembly phases were present again and the curve shifted to transitions at ∼1 M urea (Figure 4). These capsids are weaker than the untreated emulsifier dimer. This result suggests that the highly stable capsids from which these dimers were isolated were not highly enriched with subunits that would favor more of the high-urea capsids (Figure 2C). A caveat is that the dimers used in this experiment are likely to have become damaged and/or oxidized over the course of their repurification and isolation, which will affect capsid stability. A C61−C61 disulfide at the dimer interface, which oxidizes slowly in the free dimer and more rapidly in the capsid, yields a less stable capsid.[29]

Can Dimer be "Cured"? The observations in Figure 2 suggest that a small fraction of subunits could lead to defective particles. This led us to ask if it was possible to "cure" the flawed subunits. *In vitro* capsid assembly is triggered by increasing the solution ionic strength, typically through addition of NaCl, which is hypothesized to favor an assembly active form of Cp149.[6,25,26] Increasing the ionic strength also contributes to Cp149 assembly by screening electrostatic repulsion between dimers.[30] This suggests that high-NaCl assembly can lead to Cp dimers that are better at assembling. A competing effect of accelerating the assembly reaction with increasing ionic strength is the possibility of generating particles with kinetically trapped defects. Such trapped particles are particularly notable at NaCl concentrations greater than or equal to 1 M and can spontaneously anneal over time or especially at reduced ionic strength.[11,31−34] To minimize the formation of kinetic traps, particles assembled at different ionic strengths (150 mM, 300 mM, 500 mM, and 1 M) were buffer-exchanged into 300 mM NaCl before the examination of urea-induced dissociation by fluorescence (Figure 5A). The most stable capsids were assembled in 500 mM NaCl, while capsids from 150 mM NaCl were the weakest. The capsids from 150 mM NaCl dissociated completely by 3.2 M urea. The other capsid pools were shifted by ∼0.4 and ∼0.8 M urea to the right, with a fraction of

https://doi.org/10.1021/acs.biochem.1c00810
Biochemistry 2022, 61, 505−513

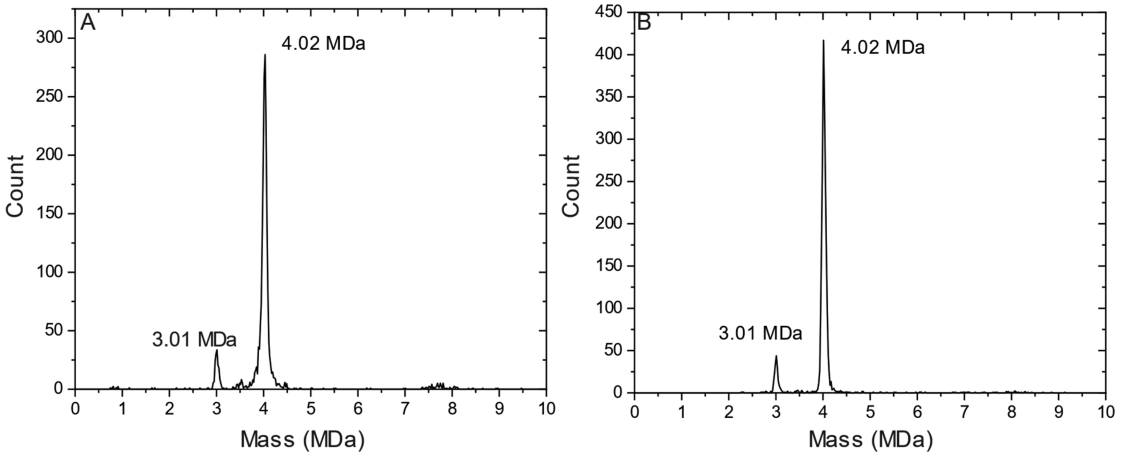

Figure 3. CDMS of Cp149 capsids before and after urea treatment. Cp149 capsids were assembled and SEC-purified in 300 mM NaCl. (A) CDMS mass distribution of untreated Cp149 capsids. The peaks at 3.01 and 4.02 MDa correspond to $T = 3$ and $T = 4$ sized particles, respectively. Note the presence of intermediates between the two peaks. (B) CDMS mass distribution of capsids incubated with 2.7 M urea for 24 h and SEC-purified. The peaks at 3.01 and 4.02 MDa correspond to $T = 3$ and $T = 4$ particles, respectively.

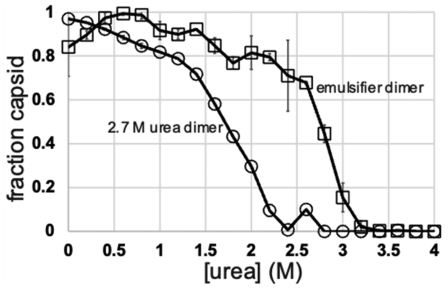

Figure 4. Disassembly of capsids made of repurified dimers isolated from 2.7 M urea capsids. Capsids assembled from the dimers of 2.7 M urea capsids were subjected to increasing urea concentrations for 24 h before quantification of capsid and dimer peaks via SEC to calculate the capsid fraction. The disassembly curve of the emulsifier dimer is also plotted for comparison.

500 mM NaCl capsids remaining until 4 M urea. A parallel SEC experiment provides essentially the same result but directly shows the loss of material from the "capsid" peak. We note that the capsid and dimer peaks had baseline separation in these experiments. In these SEC results, we also observe that capsid assembled at 1 M NaCl, which is expected to include particles with defects,[31,32] had a large fraction of particles in the low-urea phase followed by an extremely broad transition while still producing a small subset of particles that are stable up to 4 M urea. Thus, it appears that NaCl may be acting as a kosmotrope, stabilizing an assembly active state for Cp and/or allowing damaged dimers to refold.

These data led to the working hypothesis that imperfect dimers in Cp149 capsids led to the labile capsids of the low-urea phase. We sought to replicate labile capsids using deliberately flawed dimer. One approach to mimicking imperfect dimers was an assembly deficient construct, Cp149-V124A (V124A for short). V124A can assemble at a very high ionic strength or co-assemble with wild-type Cp149. The V124A mutation results in a weak association energy of approximately −2.4 kcal/contact in 300 mM NaCl (a linear extrapolation from data in ref 35). We co-assembled V124A with Cp149 at mole percentages of 1%, 10%, and 50% of V124A relative to the wild type, with pure V124A and the pure wild type as controls (Figure 6). Because it was possible that these mixed assembly reactions might exclude V124A, we purified capsids by SEC and determined the V124A mole

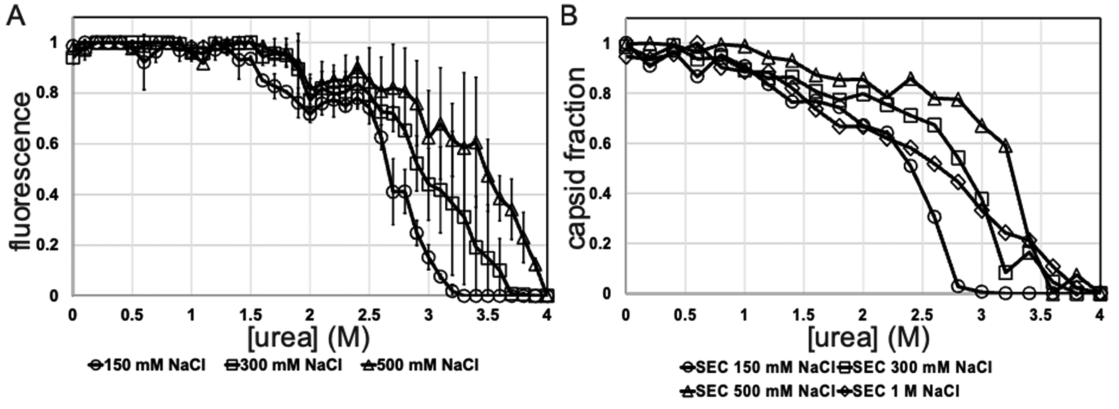

Figure 5. Capsid disassembly changes in response to the ionic strength of assembly. Cp149 capsids were assembled under a range of NaCl conditions: 150 mM (○), 300 mM (□), 500 mM (△), and 1 M (◇). The resulting capsids were SEC-purified, buffer exchanged into 300 mM NaCl, and then subjected to increasing urea concentrations for 24 h. Dissociation was evaluated by (A) intrinsic tryptophan fluorescence or (B) SEC.

https://doi.org/10.1021/acs.biochem.1c00810
Biochemistry 2022, 61, 505−513

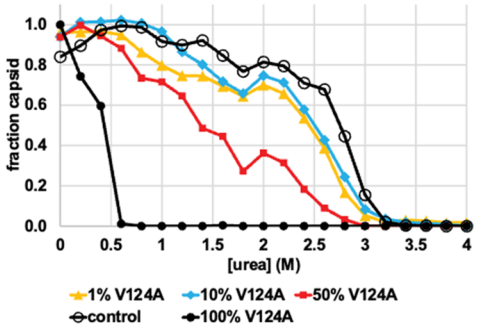

Figure 6. Disassembly of capsids co-assembled with flawed dimers. Capsids were co-assembled from a mixture of wild-type Cp149 dimers with 1%, 10%, or 50% Cp149-V124A dimers and then SEC-purified. Co-assembly was confirmed by LCMS of capsids (Table 2). A 100% V124A capsid control and a 100% wild-type Cp149 control were also SEC-purified. Each capsid pool was incubated with urea, and the resulting capsid and dimer peaks were measured by SEC (to avoid possible differences in intrinsic fluorescence) to quantify disassembly and plot the curves in the figure.

percent in capsids by LCMS (Table 2). We observed that the mutant was present in the capsid fraction at approximately the same ratio as in the initial reaction mixture.

Table 2. LCMS of Capsids in Which Cp149 and Cp149-V124A Were Co-assembled[a]

		mole percent	
dimer	peak (Da)	10% V124A co-assembly	50% V124A co-assembly
V124A homodimer	33484	11	40
wild-type Cp149	33540	89	60

[a]The LCMS produced two primary peaks, which have been assigned to Cp149 V124A and wild-type Cp149. The mole percent of each dimer species was calculated after peak integration.

In urea titrations, the 100% V124A capsids were very fragile and showed measurable dissociation under all tested urea concentrations while wild-type capsids showed the two expected phases of disassembly. The per contact association energy of the 100% V124A sample was approximately −4.6 kcal/mol. This association energy is much weaker than that observed for wild-type capsids (approximately −10 kcal/mol) but is much higher than the V124A assembly energy of −2.4 kcal/mol per contact, indicating hysteresis even in these fragile capsids. The dissociation curves for the 1% and 10% V124A capsids were nearly indistinguishable from those of wild-type capsids. Both 1% and 10% V124A had two disassembly phases that closely mirrored those of the wild type with the low-urea phase from 0.6 to 2 M urea and the high-urea phase from 2 to 3.2 M urea. In a 10% V124A capsid, on average 12 of the dimers are mutants yet the similarity of the dissociation curve indicates that dissociation is really a function of the capsid lattice and is not necessarily sensitive to the weakest link. However, for 50% V124A, a monotonic disassembly curve began at 0.6 M urea and was completed by 3 M urea. It was not clear whether there were one or two disassembly phases to the 50% V124A curve. As a summary of these experiments, small amounts of V124A are evidently tolerated in capsids without changing the dissociation curve, whereas a large fraction of V124A does weaken a capsid.

DISCUSSION

We have found that Cp149 capsids can display two disassembly phases (Figure 2). A low-urea disassembly phase lacks hysteresis as the calculated $\Delta G_{contact,disassembly}$ (−3.4 to −3.7 kcal/mol) is close to $\Delta G_{contact,assembly}$ for 300 mM NaCl (−3.5 kcal/mol). This phase correlates with a pcc of ∼5 μM dimer. The average $\Delta G_{contact,disassembly}$ for the low-urea phases in Table 1 is −3.7 ± 0.3 kcal/mol. This calculation shows that across the capsid sample types the particles in the low-urea phase appear to freely equilibrate with free dimer without detectable hysteresis. The calculation excludes 50% V124A and 100% V124A co-assembled capsids because they began dissociating at very low urea concentrations, making the measurement of a low-urea phase impossible. Capsids in the high-urea disassembly phase (Figure 2) had a $\Delta G_{contact,disassembly}$ of −10 to −14 kcal/mol corresponding to a sub-femtomolar pcc. Capsids from the second phase appear to be chemically similar to the labile capsids but are energetically quite different in their hysteresis to dissociation. The average $\Delta G_{contact,disassembly}$ for the high-urea phases in Table 1 is −10.5 ± 1.8 kcal/mol. This calculated average shows that the high-urea phase particles exhibit hysteresis irrespective of the capsid sample type (the high standard deviation is due in part to the large extrapolation to 0 M urea). An extraordinary example of the effect of hysteresis with HBV is the ability of capsids to persist for 120 days with negligible subunit exchange.[12] This heightened stability can allow capsids to persist even where they would never assemble. In the case of HBV, which assembles *in vivo* on flexible ssRNA that is then reverse transcribed into stiff dsDNA, that added stability may allow the capsid to withstand the destabilizing internal force of the packaged genome.[36]

The ratio of labile to stable capsids can be manipulated. The low-urea phase is associated with damaged capsids and damaged subunits. A very high ionic strength leads to labile capsids (Figure 5B), probably by kinetically trapping defects. A high ionic strength (where it does not lead to trapped assembly) apparently favors subunits that are more assembly competent and leads to a depletion of the low-urea phase (Figure 5). Similarly, treatment of subunits with a chaperone leads to more assembly,[37] probably by repairing misfolded Cp dimers or favoring an assembly active state. In contrast to capsids with kinetically trapped defects, capsids in the high-urea phase could be isolated by urea treatment correlated with the loss of capsids containing flaws (Figure 3).

The hysteresis we observed with wild-type Cp149 was also observed with a weakly assembling V124A mutant (Figure 6). We saw no change in disassembly when as much as 10% of the subunits were V124A. However, with 100% V124A, we observed weaker capsids that, like the wild type, had hysteresis to dissociation. Thus, dissociation and hysteresis are, at least in part, a function of the capsid lattice, not specific just to the wild-type protein.

Efforts to trap dimers that had improved assembly properties were not successful. When the urea-treated capsids were dissociated and reassembled, the resultant capsids were actually weaker than capsids of untreated, wild-type Cp149. We suspect that this was the result of Cp oxidation[29] and of damage to Cp during the lengthy isolation process, leading to the final capsids (Figure 4). "Curing" flawed subunits with NaCl acting as a kosmotropic agent was remarkably successful; independent of increasing the amount of assembly, increasing the NaCl

https://doi.org/10.1021/acs.biochem.1c00810
Biochemistry 2022, 61, 505−513

concentration from 150 to 500 mM increased the fraction of capsids in the high-urea pool (Figure 5).

With respect to the hysteresis models presented in Figure 1, it is now apparent that the capsid maturation model encompasses much of the data presented in this report (Figure 1B) while the subunit curing experiments indicate that preassembly defects and preassembly transitions can also make an important contribution. The capsid maturation model is based on a postassembly maturation transition that requires a complete capsid lattice. This model is consistent with the presence of capsids with missing subunits in the less stable (low-urea) pool, the ability of normal subunits to overwhelm a small pool of weakly assembling subunits [e.g., 10% V124A (Figure 6)], and subunits isolated from high-urea capsids did not yield intrinsically stable capsids. Conversely, the increased fraction of capsids in the high-urea pool due to assembly at a high NaCl concentration (Figure 5) and our improved purification suggests the importance of subunit structure for mature assembly. Therefore, we cannot preclude the subunit-based conformational model (Figure 1C) in concert with the capsid maturation model.

The capsid maturation model brings to mind the work of Chevreuil et al.,[38] who observed transient assembly intermediate species that were thought to be disorganized structures of Cp dimers, of $T = 4$ capsid size, which resolved into capsids through thermodynamic editing (i.e., reversible dissociation of subunits that are weakly bound because of misassembly) and self-organization. Rearrangement of overgrown or incompletely formed capsids has also been reported for HBV in CDMS studies.[31,39] This reorganization could well be a part of the path that HBV capsids take to postassembly maturation.

In summary, our data strongly support the contribution of capsid maturation to hysteresis. They are also consistent with a contribution of a subunit structural transition. Differences between the free dimer and dimer in a capsid in HBV[25] and the closely related Woodchuck hepatitis virus[40] suggest that some of the energetic difference between labile and stable capsids may arise from changes in the dynamics of the capsid, directly analogous to ensemble-based allostery.[23,41] Consistent with this proposal, molecular dynamics simulations show the HBV capsid to be highly dynamic[42] and hydrogen−deuterium exchange experiments indicate an allosteric network of hydrogen bonds that affect assembly.[43]

AUTHOR INFORMATION

Corresponding Author

Adam Zlotnick − *Department of Molecular and Cellular Biochemistry, Indiana University, Bloomington, Indiana 47405, United States;* orcid.org/0000-0001-9945-6267; Email: azlotnic@iu.edu

Authors

Caleb A. Starr − *Department of Molecular and Cellular Biochemistry, Indiana University, Bloomington, Indiana 47405, United States*

Lauren F. Barnes − *Department of Chemistry, Indiana University, Bloomington, Indiana 47405, United States*

Martin F. Jarrold − *Department of Chemistry, Indiana University, Bloomington, Indiana 47405, United States;* orcid.org/0000-0001-7084-176X

Complete contact information is available at: https://pubs.acs.org/10.1021/acs.biochem.1c00810

Funding

This work was funded by National Institutes of Health Grants R01 AI118933 to A.Z. and R01 GM129354 to Stephen Jacobson.

Notes

The authors declare the following competing financial interest(s): A.Z. has an interest in companies developing antivirals directed at the HBV capsid protein. These interests have had no impact on the design or execution of these experiments.

ACKNOWLEDGMENTS

The authors acknowledge the Laboratory for Biological Mass Spectrometry at Indiana University for assistance with LCMS. The authors also thank Kate Starr for assistance with Figure 1.

REFERENCES

(1) Venkatakrishnan, B.; Zlotnick, A. The Structural Biology of Hepatitis B Virus: Form and Function. *Annual Reviews of Virology* **2016**, *3*, 429−451.

(2) Hepatitis B Fact Sheet. World Health Organization, 2021.

(3) Zlotnick, A.; Venkatakrishnan, B.; Tan, Z.; Lewellyn, E.; Turner, W.; Francis, S. Core protein: A pleiotropic keystone in the HBV lifecycle. *Antiviral Res.* **2015**, *121*, 82−93.

(4) Rabe, B.; Delaleau, M.; Bischof, A.; Foss, M.; Sominskaya, I.; Pumpens, P.; Cazenave, C.; Castroviejo, M.; Kann, M. Nuclear entry of hepatitis B virus capsids involves disintegration to protein dimers followed by nuclear reassociation to capsids. *PLoS Pathog* **2009**, *5*, No. e1000563.

(5) Singh, S.; Zlotnick, A. Observed hysteresis of virus capsid disassembly is implicit in kinetic models of assembly. *J. Biol. Chem.* **2003**, *278*, 18249−18255.

(6) Alexander, C. G.; Jurgens, M. C.; Shepherd, D. A.; Freund, S. M.; Ashcroft, A. E.; Ferguson, N. Thermodynamic origins of protein folding, allostery, and capsid formation in the human hepatitis B virus core protein. *Proc. Natl. Acad. Sci. U. S. A.* **2013**, *110*, E2782−E2791.

(7) Zlotnick, A.; Cheng, N.; Conway, J. F.; Booy, F. P.; Steven, A. C.; Stahl, S. J.; Wingfield, P. T. Dimorphism of hepatitis B virus capsids is strongly influenced by the C-terminus of the capsid protein. *Biochemistry* **1996**, *35*, 7412−7421.

(8) Tanford, C. *The Hydrophobic Effect: Formation of Micelles and Biological Membranes*, 2nd ed.; John Wiley and Sons, Inc.: New York, 1980.

(9) Ceres, P.; Zlotnick, A. Weak protein-protein interactions are sufficient to drive assembly of hepatitis B virus capsids. *Biochemistry* **2002**, *41*, 11525−11531.

(10) Zlotnick, A. Are weak protein-protein interactions the general rule in capsid assembly? *Virology* **2003**, *315*, 269−274.

(11) Harms, Z. D.; Selzer, L.; Zlotnick, A.; Jacobson, S. C. Monitoring Assembly of Virus Capsids with Nanofluidic Devices. *ACS Nano* **2015**, *9*, 9087−9096.

(12) Uetrecht, C.; Watts, N. R.; Stahl, S. J.; Wingfield, P. T.; Steven, A. C.; Heck, A. J. Subunit exchange rates in Hepatitis B virus capsids are geometry- and temperature-dependent. *Physical chemistry chemical physics: PCCP* **2010**, *12*, 13368−13371.

(13) Creighton, T. E. *Proteins: Structures and Molecular Properties*; W. H. Freeman and Co.: New York, 1984.

(14) Zlotnick, A.; Lee, A.; Bourne, C. R.; Johnson, J. M.; Domanico, P. L.; Stray, S. J. In vitro screening for molecules that affect virus capsid assembly (and other protein association reactions). *Nat. Protoc* **2007**, *2*, 490−498.

(15) Contino, N. C.; Jarrold, M. F. Charge detection mass spectrometry for single ions with a limit of detection of 30 charges. *Int. J. Mass Spectrom.* **2013**, *345*−*347*, 153−159.

(16) Keifer, D.; Pierson, E.; Jarrold, M. F. Charge detection mass spectrometry: Weighing heavier things. *Analyst* **2017**, *142*, 1654−1671.

(17) Draper, B. E.; Anthony, S. N.; Jarrold, M. F. The FUNPET-a New Hybrid Ion Funnel-Ion Carpet Atmospheric Pressure Interface for the Simultaneous Transmission of a Broad Mass Range. *J. Am. Soc. Mass Spectrom.* **2018**, *29*, 2160−2172.
(18) Draper, B. E.; Jarrold, M. F. Real-Time Analysis and Signal Optimization for Charge Detection Mass Spectrometry. *J. Am. Soc. Mass Spectrom.* **2019**, *30*, 898−904.
(19) Zlotnick, A. To build a virus capsid. An equilibrium model of the self assembly of polyhedral protein complexes. *J. Mol. Biol.* **1994**, *241*, 59−67.
(20) Prevelige, P. E.; Fane, B. A. Building the machines: scaffolding protein functions during bacteriophage morphogenesis. *Adv. Exp. Med. Biol.* **2012**, *726*, 325−350.
(21) Black, L. W.; Rao, V. B. Structure, assembly, and DNA packaging of the bacteriophage T4 head. *Adv. Virus Res.* **2012**, *82*, 119−153.
(22) Duda, R. L.; Teschke, C. M. The amazing HK97 fold: versatile results of modest differences. *Curr. Opin Virol* **2019**, *36*, 9−16.
(23) Hilser, V. J.; Wrabl, J. O.; Motlagh, H. N. Structural and energetic basis of allostery. *Annu. Rev. Biophys* **2012**, *41*, 585−609.
(24) Steven, A. C.; Carrascosa, J. L. Proteolytic cleavage and structural transformation: their relationship in bacteriophage T4 capsid maturation. *J. Supramol. Struct.* **1979**, *10*, 1−11.
(25) Packianathan, C.; Katen, S. P.; Dann, C. E.; Zlotnick, A. Conformational changes in the Hepatitis B virus core protein are consistent with a role for allostery in virus assembly. *J. Virol* **2010**, *84*, 1607−1615.
(26) Stray, S. J.; Ceres, P.; Zlotnick, A. Zinc ions trigger conformational change and oligomerization of hepatitis B virus capsid protein. *Biochemistry* **2004**, *43*, 9989−9998.
(27) Lazaro, G. R.; Hagan, M. F. Allosteric Control of Icosahedral Capsid Assembly. *J. Phys. Chem. B* **2016**, *120*, 6306−6318.
(28) Zhao, Z.; Wang, J. C.; Segura, C. P.; Hadden-Perilla, J. A.; Zlotnick, A. The Integrity of the Intradimer Interface of the Hepatitis B Virus Capsid Protein Dimer Regulates Capsid Self-Assembly. *ACS Chem. Biol.* **2020**, *15*, 3124−3132.
(29) Selzer, L.; Katen, S. P.; Zlotnick, A. The hepatitis B virus core protein intradimer interface modulates capsid assembly and stability. *Biochemistry* **2014**, *53*, 5496−5504.
(30) Kegel, W. K.; van der Schoot, P. Competing hydrophobic and screened-coulomb interactions in hepatitis B virus capsid assembly. *Biophys. J.* **2004**, *86*, 3905−3913.
(31) Lutomski, C. A.; Lyktey, N. A.; Zhao, Z.; Pierson, E. E.; Zlotnick, A.; Jarrold, M. F. Hepatitis B Virus Capsid Completion Occurs through Error Correction. *J. Am. Chem. Soc.* **2017**, *139*, 16932−16938.
(32) Pierson, E. E.; Keifer, D. Z.; Selzer, L.; Lee, L. S.; Contino, N. C.; Wang, J. C.; Zlotnick, A.; Jarrold, M. F. Detection of late intermediates in virus capsid assembly by charge detection mass spectrometry. *J. Am. Chem. Soc.* **2014**, *136*, 3536−3541.
(33) Asor, R.; Selzer, L.; Schlicksup, C. J.; Zhao, Z.; Zlotnick, A.; Raviv, U. Assembly Reactions of Hepatitis B Capsid Protein into Capsid Nanoparticles Follow a Narrow Path through a Complex Reaction Landscape. *ACS Nano* **2019**, *13*, 7610−7626.
(34) Asor, R.; Schlicksup, C. J.; Zhao, Z.; Zlotnick, A.; Raviv, U. Rapidly Forming Early Intermediate Structures Dictate the Pathway of Capsid Assembly. *J. Am. Chem. Soc.* **2020**, *142*, 7868−7882.
(35) Tan, Z.; Pionek, K.; Unchwaniwala, N.; Maguire, M. L.; Loeb, D. D.; Zlotnick, A. The Interface between Hepatitis B Virus Capsid Proteins Affects Self-Assembly, Pregenomic RNA Packaging, and Reverse Transcription. *J. Virol* **2015**, *89*, 3275−3284.
(36) Dhason, M. S.; Wang, J. C.; Hagan, M. F.; Zlotnick, A. Differential assembly of Hepatitis B Virus core protein on single- and double-stranded nucleic acid suggest the dsDNA-filled core is spring-loaded. *Virology* **2012**, *430*, 20−29.
(37) Shim, H. Y.; Quan, X.; Yi, Y. S.; Jung, G. Heat shock protein 90 facilitates formation of the HBV capsid via interacting with the HBV core protein dimers. *Virology* **2011**, *410*, 161−169.
(38) Chevreuil, M.; Lecoq, L.; Wang, S.; Gargowitsch, L.; Nhiri, N.; Jacquet, E.; Zinn, T.; Fieulaine, S.; Bressanelli, S.; Tresset, G. Nonsymmetrical Dynamics of the HBV Capsid Assembly and Disassembly Evidenced by Their Transient Species. *J. Phys. Chem. B* **2020**, *124*, 9987−9995.
(39) Pierson, E.; Keifer, D. Z.; Kukreja, A. A.; Wang, J. C.-Y.; Zlotnick, A.; Jarrold, M. F. Charge Detection Mass Spectrometry Identifies Preferred Non-Icosahedral Polymorphs in the Self-Assembly of Woodchuck Hepatitis Virus Capsids. *J. Mol. Biol.* **2016**, *428*, 292−300.
(40) Zhao, Z.; Wang, J. C.; Gonzalez-Gutierrez, G.; Venkatakrishnan, B.; Asor, R.; Khaykelson, D.; Raviv, U.; Zlotnick, A. Structural Differences between the Woodchuck Hepatitis Virus Core Protein in the Dimer and Capsid States Are Consistent with Entropic and Conformational Regulation of Assembly. *J. Virol.* **2019**, *93*, No. e00141-00119.
(41) Motlagh, H. N.; Wrabl, J. O.; Li, J.; Hilser, V. J. The ensemble nature of allostery. *Nature* **2014**, *508*, 331−339.
(42) Hadden, J. A.; Perilla, J. R.; Schlicksup, C. J.; Venkatakrishnan, B.; Zlotnick, A.; Schulten, K. All-atom molecular dynamics of the HBV capsid reveals insights into biological function and cryo-EM resolution limits. *eLife* **2018**, *7*, 7.
(43) Patterson, A.; Zhao, Z.; Waymire, E.; Zlotnick, A.; Bothner, B. Dynamics of Hepatitis B Virus Capsid Protein Dimer Regulate Assembly through an Allosteric Network. *ACS Chem. Biol.* **2020**, *15*, 2273−2280.

https://doi.org/10.1021/acs.biochem.1c00810
Biochemistry 2022, 61, 505−513